This is a repository copy of *Signatures of the $d^*(2380)$ hexaquark in d(γ,$p\vec{n}$)*.

White Rose Research Online URL for this paper:
https://eprints.whiterose.ac.uk/id/eprint/159214/

Version: Published Version

Signatures of the $d^*(2380)$ Hexaquark in $d(\gamma, p\vec{n})$

M. Bashkanov[1] D. P. Watts,[1,*] S. J. D. Kay,[2] S. Abt,[3] P. Achenbach,[4] P. Adlarson,[4] F. Afzal,[5] Z. Ahmed,[2] C. S. Akondi,[6] J. R. M. Annand,[7] H. J. Arends,[4] R. Beck,[5] M. Biroth,[4] N. Borisov,[8] A. Braghieri,[9] W. J. Briscoe,[10] F. Cividini,[4] C. Collicott,[11] S. Costanza,[12,9] A. Denig,[4] E. J. Downie,[10] P. Drexler,[4,13] S. Fegan,[1] A. Fix,[14] S. Gardner,[7] D. Ghosal,[3] D. I. Glazier,[7] I. Gorodnov,[8] W. Gradl,[4] M. Günther,[3] D. Gurevich,[15] L. Heijkenskjöld,[4] D. Hornidge,[16] G. M. Huber,[2] A. Käser,[3] V. L. Kashevarov,[4,8] M. Korolija,[17] B. Krusche,[3] A. Lazarev,[8] K. Livingston,[7] S. Lutterer,[3] I. J. D. MacGregor,[7] D. M. Manley,[6] P. P. Martel,[4,16] R. Miskimen,[18] E. Mornacchi,[4] C. Mullen,[7] A. Neganov,[8] A. Neiser,[4] M. Ostrick,[4] P. B. Otte,[4] D. Paudyal,[2] P. Pedroni,[9] A. Powell,[7] S. N. Prakhov,[19] G. Ron,[20] A. Sarty,[11] C. Sfienti,[4] V. Sokhoyan,[4] K. Spieker,[5] O. Steffen,[4] I. I. Strakovsky,[10] T. Strub,[3] I. Supek,[17] A. Thiel,[5] M. Thiel,[4] A. Thomas,[4] Yu. A. Usov,[8] S. Wagner,[4] N. K. Walford,[3] D. Werthmüller,[1] J. Wettig,[4] M. Wolfes,[4] N. Zachariou,[1] and L. A. Zana[21]

(A2 Collaboration at MAMI)

[1]*Department of Physics, University of York, Heslington, York Y010 5DD, United Kingdom*
[2]*University of Regina, Regina, SK S4S0A2 Canada*
[3]*Department of Physics, University of Basel, Ch-4056 Basel, Switzerland*
[4]*Institut für Kernphysik, University of Mainz, D-55099 Mainz, Germany*
[5]*Helmholtz-Institut für Strahlen- und Kernphysik, University Bonn, D-53115 Bonn, Germany*
[6]*Kent State University, Kent, Ohio 44242, USA*
[7]*SUPA School of Physics and Astronomy, University of Glasgow, Glasgow G12 8QQ, United Kingdom*
[8]*Joint Institute for Nuclear Research, 141980 Dubna, Russia*
[9]*INFN Sezione di Pavia, I-27100 Pavia, Pavia, Italy*
[10]*Center for Nuclear Studies, The George Washington University, Washington, DC 20052, USA*
[11]*Department of Astronomy and Physics, Saint Mary's University, E4L1E6 Halifax, Canada*
[12]*Dipartimento di Fisica, Università di Pavia, I-27100 Pavia, Italy*
[13]*II. Physikalisches Institut, University of Giessen, D-35392 Giessen, Germany*
[14]*Tomsk Polytechnic University, 634034 Tomsk, Russia*
[15]*Institute for Nuclear Research, RU-125047 Moscow, Russia*
[16]*Mount Allison University, Sackville, New Brunswick E4L1E6, Canada*
[17]*Rudjer Boskovic Institute, HR-10000 Zagreb, Croatia*
[18]*University of Massachusetts, Amherst, Massachusetts 01003, USA*
[19]*University of California Los Angeles, Los Angeles, California 90095-1547, USA*
[20]*Racah Institute of Physics, Hebrew University of Jerusalem, Jerusalem 91904, Israel*
[21]*Thomas Jefferson National Accelerator Facility, Newport News, Virginia 23606, USA*

We report a measurement of the spin polarization of the recoiling neutron in deuterium photodisintegration, utilizing a new large acceptance polarimeter within the Crystal Ball at MAMI. The measured photon energy range of 300–700 MeV provides the first measurement of recoil neutron polarization at photon energies where the quark substructure of the deuteron plays a role, thereby providing important new constraints on photodisintegration mechanisms. A very high neutron polarization in a narrow structure centered around $E_\gamma \sim 570$ MeV is observed, which is inconsistent with current theoretical predictions employing nucleon resonance degrees of freedom. A Legendre polynomial decomposition suggests this behavior could be related to the excitation of the $d^*(2380)$ hexaquark.

Introduction.—The photodisintegration of the deuteron is one of the simplest reactions in nuclear physics, in which a well understood and clean electromagnetic probe leads to the breakup of a few-body nucleonic system. However, despite experimental measurements of deuteron photodisintegration spanning almost a century [1], many key experimental observables remain unmeasured. This is particularly evidenced at distance scales (photon energies) where the quark substructure of the deuteron can be excited. This limits a detailed assessment of the reaction mechanism, including the contributions of nucleon resonances and meson exchange currents as well as potential roles for more exotic QCD possibilities, such as the six-quark containing (hexaquark) $d^*(2380)$ recently evidenced in a range of nucleon-nucleon scattering reactions [2–9]. The $d^*(2380)$ has inferred quantum numbers $I(J^P) = 0(3^+)$ and a mass ~ 2380 MeV, which in photoreactions would correspond to a pole at $E_\gamma \sim 570$ MeV. Constraints on the existence, properties [10] and electromagnetic coupling of the $d^*(2380)$ would have important ramifications for the emerging field of nonstandard multiquark states and our understanding of the dynamics of condensed matter systems such as neutron stars [11].

Although cross sections for deuterium photodisintegration have been determined [12], polarization observables provide different sensitivities to the underlying reaction processes and are indispensable in constraining the basic photoreaction amplitudes. Of all the single-polarization variables, the ejected nucleon polarization (P_y) is probably the most challenging experimentally, requiring the characterization of a sufficient statistical quantity of events where the ejectile nucleon subsequently undergoes a (spin-dependent) nuclear scattering reaction in an analyzing medium. Nucleon polarization measurements of sufficient quality have therefore only recently become feasible with the availability of sufficiently intense photon beams. Efforts to date have focused on recoil proton polarization (P_y^p) [13,14], exploiting proton polarimeters in the focal planes of (small acceptance) magnetic spectrometers. The data have good statistical accuracy but with a discrete and sparse coverage of incident photon energy and breakup kinematics [13,14], with most data restricted to a proton polar angle of $\Theta_p^{c.m.} \sim 90°$ in the photon-deuteron center-of-mass (c.m.) frame. However, these available P_y^p data do exhibit a distinct behavior, reaching ~ -1 (i.e., around -100% polarization), in a narrow structure centered on $E_\gamma \sim 550$ MeV. Because of the inability to describe this behavior with theoretical calculations including only the established nucleon resonances, it was speculated [13,15] that it would be consistent with a then unknown 6-quark resonance, with inferred properties having a striking similarity to the $d^*(2380)$ hexaquark discovered later in NN scattering.

Clearly, measurement of the ejected neutron polarization (P_y^n) would be important to establish a role for the $d^*(2380)$ in photodisintegration. In $d^*(2380) \rightarrow pn$ decays, the spins of the proton and neutron would be expected to be aligned [16]. Therefore, if the P_y^p anomaly originates from a $d^*(2380)$ contribution, the neutron polarization should mimic this anomalous behavior. Measurements of P_y^n are even more challenging experimentally than P_y^p, due to the inability to track the uncharged neutron into the scattering medium, and have only been obtained below $E_\gamma \sim 30$ MeV [17,18]. The experimental difficulties even led to attempts to extract P_y^n from studies of the inverse reaction $\vec{n} + p \rightarrow d + \gamma$, using detailed balance [19,20].

This new work provides the first measurement of P_y^n in deuterium photodisintegration for E_γ sensitive to the quark substructure of the deuteron, covering $E_\gamma = 300–700$ MeV and neutron breakup angles in the photon-deuteron c.m. frame of $\Theta_n^{c.m.} = 60°–120°$.

Experimental details.—The measurement employed a new large acceptance neutron polarimeter [21] within the Crystal Ball detector at the A2@MAMI [22] facility during a 300 h beam time. An 1557 MeV longitudinally polarized electron beam impinged on either a thin amorphous (cobalt-iron alloy) or crystalline (diamond) radiator, producing circularly (alloy) or linearly (diamond) polarized bremsstrahlung photons. As photon beam polarization is not used to extract P_y^n, equal flux from the two linear or circular polarization settings were combined to increase the unpolarized yield. The photons were energy-tagged ($\Delta E \sim 2$ MeV) by the Glasgow-Mainz Tagger [23] and impinged on a 10 cm long liquid deuterium target cell. Reaction products were detected by the Crystal Ball (CB) [24], a highly segmented NaI(Tl) photon calorimeter covering nearly 96% of 4π steradians. For this experiment, a new bespoke 24 element, 7 cm diam and 30 cm long plastic scintillator barrel (PID-POL) [25] surrounded the target, with a smaller diameter than the earlier PID detector [25], but provided similar particle identification capabilities. A 2.6 cm thick cylinder of analyzing material (graphite) for nucleon polarimetry was placed around PID-POL, covering polar angles $12° < \theta < 150°$ and occupying the space between PID-POL and the multiwire proportional chamber (MWPC) [26]. The MWPC provided charged particle tracking for particles passing out of the graphite into the CB. At forward angles, an additional 2.6 cm thick graphite disc covered the range $2 < \theta < 12°$ [25,27].

The $d(\gamma, p\vec{n})$ events of interest consist of a primary proton track and a reconstructed neutron, which undergoes a (n, p) charge-exchange reaction in the graphite to produce a secondary proton which gives signals in the MWPC and CB. The primary proton was identified using the correlation between the energy deposits in the PID and CB using $\Delta E - E$ analysis [25] along with an associated charged track in the MWPC. The intercept of the primary proton track with the photon beam line allowed determination of the production vertex, and hence permitted the yield originating from the target cell windows to be

removed. Neutron $^{12}C(n,p)$ charge exchange candidates required an absence of a PID-POL signal on the reconstructed neutron path, while having an associated track in the MWPC and signal in the CB from the scattered secondary proton. The incident neutron angle (θ_n) was determined using E_γ and the production vertex coordinates. A distance of closest approach condition was imposed to ensure a crossing of the (reconstructed) neutron track and the secondary proton candidate track (measured with MWPC and CB). Once candidate proton and neutron tracks were identified, a kinematic fit was employed to increase the sample purity and improve the determination of the reaction kinematics [28], exploiting the fact that the disintegration can be constrained with measurements of two kinematic quantities while three (θ_p, T_p and θ_n) are measured in the experiment. A 10% cut on the probability function was used to select only events from the observed uniform probability region [29].

Determination of neutron polarization.—The neutron polarization was determined through analysis of the neutron-spin dependent $^{12}C(n,p)$ reactions occurring in the graphite polarimeter. The spin-orbit component of the nucleon-nucleon interaction results in a ϕ anisotropy in the produced yield of secondary protons. For a fixed nucleon energy, the secondary proton yield as a function of polar (Θ) and azimuthal (ϕ) scattering angle can be expressed as

$$N(\Theta,\phi)^{\text{pol}} = N(\Theta,\phi)^{\text{unpol}}[1 + P_n A_y(\Theta)\cos(\phi)], \quad (1)$$

where P_n is the neutron polarization and A_y is the analyzing power. A_y for free $n-p$ scattering is established for the appropriate energy range in the SAID parametrization [30]. Differences in the analyzing power between the free (n,p) process and the in-medium $^{12}C(n,p)X$ process were established by a direct measurement of A_y for $^{12}C(n,p)X$ by JEDI@Juelich [31]. Above $T_n = 300$ MeV the measured A_y agreed with the SAID (n,p) parametrization to within a few percent. For lower energies, the influence of coherent nuclear processes, such as $^{12}C(n,p)^{12}N$ resulted in an increased magnitude (around a factor of 2) but exhibiting a similar Θ dependence to the free reaction [27]. The (n,p) analyzing power from SAID was corrected [32] by the function

$$A_y(n^{12}C)/A_y(np) = 1 + e^{(1.82-0.014E_n[\text{MeV}])}. \quad (2)$$

To reduce systematic dependencies in the simulation of the polarimeter the events were only retained if $A_y(np)$ was above 0.1, the proton scattering angle (Θ) was in the range $\Theta_p^{\text{scat}} \in 15 - 45°$ and $\Theta_n - \Theta_p^{\text{scat}} > 27°$ where Θ_p^{scat} is the polar angle of scattered proton relative to the direction of the neutron. The latter cut reduced the contribution of secondary protons traveling parallel to the axis of the
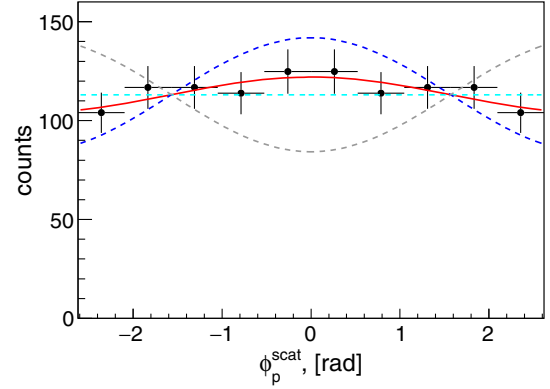

FIG. 1. The measured ϕ_p^{scat} distribution (corrected for efficiency and acceptance) for $E_\gamma = 350$ MeV and $\Theta_n^{\text{c.m.}} = 90°$. The red line shows the fit [Eq. (1)], giving $P_y = -0.31 \pm 0.18$. The cyan, blue, and gray dashed lines correspond to $P_y = 0, -1$, and 1, respectively. All fits are for $A_y = -0.25$.

polarimeter. The scattered yields were corrected for small angle-dependent variations in detection efficiency from the MWPC, established using reconstructed charged particles in the data. The acceptance with the above cuts was determined using a GEANT4 [33] simulation of the apparatus. The yield of scattered events was then corrected for this efficiency and the polarization extracted according to Eq. (1). An example of the measured distribution and the fits to extract P_y^n are shown in Fig. 1.

To quantify systematic errors in the P_y^n extraction, the analysis cuts were relaxed. This involved widening the cuts on the scattered proton angle and minimum energy (both of which change the MWPC efficiency), reducing the minimum analyzing power cut, as well as varying the minimum probability in the kinematic fit up to 40% [27]. The systematic errors are extracted from the resulting variations in the extracted P_y^n, so include significant contributions from the achievable measurement statistics. The main systematic error arose from variations in the ϕ-dependent detector efficiencies for the secondary protons in GEANT4, which had increasing influence for the lower nucleon energies. The extracted systematic error in P_y^n was typically around ± 0.2 and is presented bin by bin with the results in the next section.

Results.—The extracted P_y^n are presented as a function of photon energy at a fixed $\theta_n^{\text{c.m.}} \sim 90°$ bin in Fig. 2. The P_y^n observable was extracted in both a binned (red-filled circles) and an unbinned (black dashed line) ansatz. Both methods gave consistent results within the statistical accuracy of the data. At the lower photon energies, in the region of the Δ resonance, P_y^n is negative in sign, small in magnitude and rather uniform. However, at higher photon energies the P_y^n data exhibit a pronounced and sharp structure reaching ~ -1 around $E_\gamma \sim 550$ MeV. The new data reveal a striking consistency between P_y^n and the previous P_y^p [13] measurements (blue open circles) in the region of the $d^*(2380)$.
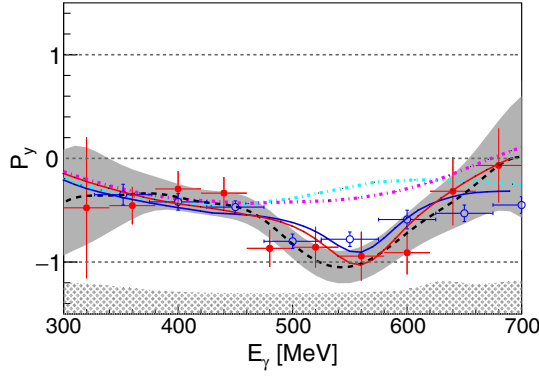
FIG. 2. P_y^n (Red filled circles) and previous P_y^p [13] (blue open circles) for c.m. angular bins centered on 90° as a function of photon energy. The result of an unbinned analysis of P_y^n is presented as a black dashed line with the error bars as a gray band. The dashed-dotted lines show predictions from Ref. [34] for P_y^p (cyan) and P_y^n (pink). The solid lines show the result of the fit with an additional $d^*(2380)$ contribution (see text) for P_y^p (blue) and P_y^n (red). Systematic uncertainties for the P_y^n data are shown by the hatched area.

The cyan (pink) dashed-dot curves show theoretical calculations of P_y^p (P_y^n), respectively. The model includes meson exchange currents (π, ρ, η, ω) and conventional nucleon resonance degrees of freedom [34]. These calculations reproduce the measured P_y^p and P_y^n in the Δ region, but fail to describe the pronounced and narrow structure centred around $E_\gamma \sim 550$ MeV for either observable. At the very highest photon energies the model predictions are consistent with the trend towards smaller P_y^n and P_y^p shown by the data. For the very highest bins P_y^n and P_y^p are predicted to diverge, attributed [34] to the $N^*(1520)$ resonance having opposite sign for photocoupling to the neutron and proton [35]. Although these differences are consistent with the current data, future experiments with improved statistical accuracy would be essential to resolve this question.

The blue (red) solid lines show a simple approximation to include an additional contribution to these theoretical predictions from the $d^*(2380)$ hexaquark in P_y^n (P_y^p), taking the established mass and width, and having a magnitude fitted to reproduce the P_y^p data alone. Previous observations of a lack of mixing of the $d^*(2380)$ with nucleon resonance backgrounds in the inverted reaction $\vec{n}p \rightarrow d^*$ gives some justification to this approximate ansatz [8,9].

The main features of the data in the $d^*(2380)$ region, specifically the minima position and width of the dip evident in both P_y^n and P_y^p, appear consistent with a $d^*(2380)$ contribution of a common magnitude for both channels. Such a common magnitude may be expected from a symmetric decay to pn from a particle which does not mix significantly with other [non-$d^*(2380)$] background contributions. Clearly, more detailed theoretical calculations including the $d^*(2380)$ in a consistent

framework within the model would be a valuable next step and we hope our new results will encourage such efforts.

The new dataset also has sufficient kinematic acceptance and statistical accuracy to provide a first measurement of the angular dependence of P_y^n. For a $d^*(2380) \rightarrow pn$ decay, P_y^n would be expected to exhibit the angular behavior of the associated P_1^3 Legendre function [36], reaching a maximum at $\theta_n^{c.m.} = 90°$ with zero crossings at $\theta_n^{c.m.} = 64°$ and 116°. In Fig. 3, P_y^n is presented as a function of $\theta_n^{c.m.}$ for two E_γ bins, in the Δ region and in the region of the $d^*(2380)$. The P_y^n data from the Δ region show a broadly flat distribution for most of the $\theta_n^{c.m.}$ range, although with a diminishing statistical definition near the edge of the polarimeter acceptance [37]. The previous P_y^p data (open points) show general agreement with P_y^n, as also predicted by the model [34]. In the $d^*(2380)$ region, P_y^n has larger magnitude and exhibits a distinct angular dependence, with a minima of ~ -1 reached at $\sim 90°$. The single datum for P_y^p in this bin (open point) also appears consistent with the new P_y^n determination.

To quantify the dependence of P_y^n on photon energy and polar angle, we performed an expansion of our results into associated Legendre functions.
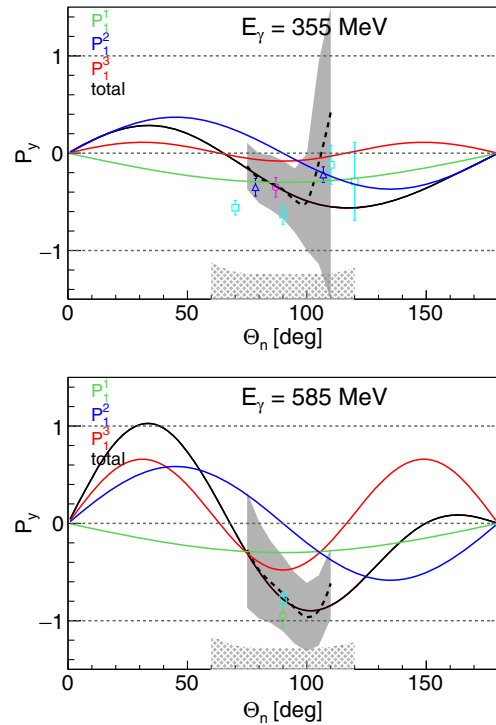

FIG. 3. P_y^n is presented as a black dashed line with the error bars as a gray band (unbinned ansatz) as a function of $\theta_n^{c.m.}$ for E_γ bins centered on 355 (upper) and 585 MeV (lower). Existing P_y^p data are shown as open symbols: cyan squares [13], pink circle [38], blue triangles [39], and green circle [14]. The curves are results of the Legendre decomposition (see text): $a_1 P_1^1$ (green), $a_2 P_1^2$ (blue), $a_3 P_1^3$ (red), and their sum (black). Systematic uncertainty is shown as the hatched area.
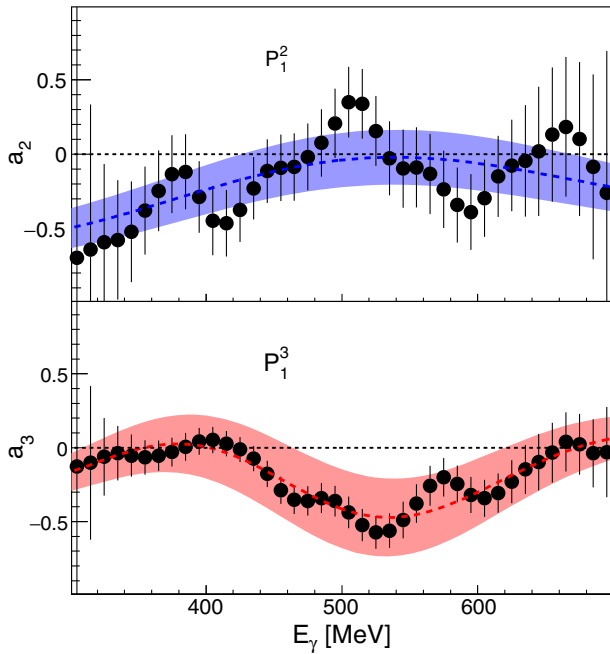
FIG. 4. Legendre polynomial decomposition of neutron polarization. P_1^2 (top) and P_1^3 (bottom). The P_1^1 contribution was fixed to constant value -0.3. The black markers correspond to single energy solutions. The dotted lines represent energy-dependent solutions, with fit errors shown by the colored bands.

$$P_y^n = \sum_{l=1}^{3} a_l P_1^l. \qquad (3)$$

The result of this expansion can be seen in Fig. 3, which shows the fitted contributions from $a_1 P_1^1$ (green line), $a_2 P_1^2$ (blue line), and $a_3 P_1^3$ (red line), and the sum of all contributions (black line). The strongly varying angular behavior in the $d^*(2380)$ region is consistent with a sizable P_1^3 contribution [40].

Figure 4 shows the E_γ dependence of fitted expansion coefficients. We employ the prescription adopted in Ref. [29] and use two fit methods: (i) a single-energy procedure in which the fit was performed using data from each photon energy bin in isolation (black data points) and (ii) an energy-dependent procedure where the expansion coefficients, a_l, were assumed to vary smoothly from bin to bin (dotted lines with the errors represented by bands). The a_1 coefficient did not show any particular energy dependent variation, so it was fixed to the value of $a_1 = -0.3$ [41]. The extracted coefficients are presented as a function of photon energy in Fig. 4. The energy dependence of the P_1^3 coefficient is consistent with the established mass and width of the $d^*(2380)$ hexaquark ($M = 2380 \pm 10$ and $\Gamma = 70 \pm 10$ MeV), indicating the angular dependence of P_y^n is consistent with a sizable $J = 3$ contribution having properties consistent with those of the $d^*(2380)$.

Summary.—The recoil neutron polarization in deuteron photodisintegration has been measured for
$300 < E_\gamma < 700$ MeV and photon-deuteron center-of-mass breakup angles for the proton of $60°$–$120°$, providing the first measurement of this fundamental observable at photon energies where the quark substructure of the deuteron can play a role in the mechanism. At lower photon energies, the data are well described by a reaction model which includes meson exchange currents and the known nucleon resonances. At higher photon energies, a narrow structure centered around $E_\gamma \sim 550$ MeV is observed in which the neutrons reach a high polarization. Such behavior is not reproduced by the theoretical model and is consistent with the "anomalous" structure observed previously for the recoil proton polarization [13]. In a simple ansatz the photon energy and angular dependencies of this "anomaly" are consistent with a contribution from the $J^p = 3^+$ $d^*(2380)$ hexaquark.

[*] daniel.watts@york.ac.uk

[1] J. Chadwick and M. Goldhaber, Nature (London) **134**, 237 (1934).
[2] M. Bashkanov, C. Bargholtz, M. Berlowski, D. Bogoslawsky, H. Calen *et al.*, Phys. Rev. Lett. **102**, 052301 (2009).
[3] P. Adlarson *et al.*, Phys. Rev. Lett. **106**, 242302 (2011).
[4] P. Adlarson *et al.*, Phys. Lett. B **721**, 229 (2013).
[5] P. Adlarson *et al.*, Phys. Rev. C **88**, 055208 (2013).
[6] P. Adlarson *et al.*, Phys. Lett. B **743**, 325 (2015).
[7] P. Adlarson *et al.*, Eur. Phys. J. A **52**, 147 (2016).
[8] P. Adlarson *et al.*, Phys. Rev. Lett. **112**, 202301 (2014).
[9] P. Adlarson *et al.*, Phys. Rev. C **90**, 035204 (2014).
[10] M. Bashkanov, H. Clement, and T. Skorodko, Eur. Phys. J. A **51**, 87 (2015).
[11] I. Vidaña, M. Bashkanov, D. P. Watts, and A. Pastore, Phys. Lett. B **781**, 112 (2018).
[12] R. Crawford *et al.*, Nucl. Phys. **A603**, 303 (1996).
[13] H. Ikeda *et al.*, Phys. Rev. Lett. **42**, 1321 (1979).
[14] K. Wijesooriya *et al.*, Phys. Rev. Lett. **86**, 2975 (2001).
[15] T. Kamae and T. Fujita, Phys. Rev. Lett. **38**, 471 (1977).
[16] The spin 3 nature of the $d^*(2380)$ requires high partial waves in the decay to a proton-neutron final state [8,9].

In 90% of cases this is via the $^3D_3$ partial wave (angular momentum $L = 2$, nucleon spins and L all aligned) or in 10% of cases via the $^3G_3$ partial wave (angular momentum $L = 4$, nucleon spins aligned, spin and L anti-aligned).

[17] D. E. Frederick, Phys. Rev. **130**, 1131 (1963).

[18] W. Bertozzi, P. T. Demos, S. Kowalski, C. P. Sargent, W. Turchinetz, R. Fullwood, and J. Russell, Phys. Rev. Lett. **10**, 106 (1963).

[19] M. Hugi et al., Nucl. Phys. **A472**, 701 (1987).

[20] J. M. Cameron et al., Nucl. Phys. **A458**, 637 (1986).

[21] D. P. Watts, J. R. M Annand, M. Bashkanov, and D. I. Glazier, MAMI Proposal Nr. A2/03-09, http://bamboo.pv .infn.it/Mambo/MAMI/prop_2009/MAMI-A2-03-09.pdf.

[22] K.-H. Kaiser et al., Nucl. Instrum. Methods Res., Phys. Res., Sect. A **593**, 159 (2008).

[23] J. C. McGeorge et al., Eur. Phys. J. A **37**, 129 (2008).

[24] A. Starostin, B. M. K. Nefkens, E. Berger, M. Clajus, A. Marusic et al., Phys. Rev. C **64**, 055205 (2001).

[25] S. J. D. Kay, Ph.D. thesis, University of Edinburgh, 2018, https://www.era.lib.ed.ac.uk/handle/1842/31525.

[26] G. Audit et al., Nucl. Instrum. Methods Res., Phys. Res., Sect. A **301**, 473 (1991).

[27] M. Bashkanov et al. (to be published).

[28] With photon energy treated as fixed, primary proton–measured, primary neutron unmeasured.

[29] M. Bashkanov et al., Phys. Lett. B **789**, 7 (2019).

[30] SAID database http://gwdac.phys.gwu.edu/; R. A. Arndt, W. J. Briscoe, I. I. Strakovsky, and R. L. Workman, Phys. Rev. C **76**, 025209 (2007).

[31] http://collaborations.fz-juelich.de/ikp/jedi/.

[32] Note that for the nucleon energies analyzed in this experiment the potential contribution of inelastic processes in which an additional pion is produced in the final state are negligible.

[33] S. Agostinelli et al., Phys. Res. A **506**, 250 (2003).

[34] Y. Kang, Ph.D. thesis, University of Bonn, Bonn, 1993.

[35] J. Babcock and J. L. Rosner, Ann. Phys. (Leipzig) **96**, 19 (1976).

[36] Such analogous polarization dependencies have already been exploited in $\vec{n}p$-elastic scattering but in the inverse direction Refs. [8,9], providing key indications of the existence of $d^*(2380)$ in NN scattering.

[37] The poor statistical accuracy for these data at the edge of the polarimeter acceptance arises from a combination of the smaller cross section at backward angles and from such low energy neutrons having diminishing (n, p) scatter acceptance and analyzing power.

[38] A. S. Bratashevski et al., Pis'ma Zh. Eksp. Teor. Fiz. **31**, 295 (1980).

[39] F. F. Liu, D. E. Lundquist, and B. H. Wiik, Phys. Rev. **165**, 1478 (1968).

[40] Note the P_1^2 term is exactly zero at 90° so the energy dependence of Fig. 2 corresponds to the sum P_1^1 and P_1^3 only.

[41] The current data does not have the statistical accuracy to effectively constrain a three-parameter fit, in which a_1 is an additional degree of freedom to a_2 and a_3. However, such fits did give consistent results, albeit with larger errors.